FULL PAPER

Dalton
www.rsc.org/dalton

Synthesis and characterisation of some new boron compounds containing the 2,4,6-$(CF_3)_3C_6H_2$ (fluoromes = Ar), 2,6-$(CF_3)_2C_6H_3$ (fluoroxyl = Ar′), or 2,4-$(CF_3)_2C_6H_3$ (Ar″) ligands †

Stéphanie M. Cornet, Keith B. Dillon,* Christopher D. Entwistle, Mark A. Fox,* Andrés E. Goeta, Helen P. Goodwin, Todd B. Marder and Amber L. Thompson
Chemistry Department, University of Durham, South Road, Durham, UK DH1 3LE. E-mail: k.b.dillon@durham.ac.uk

Received 14th August 2003, Accepted 4th September 2003
First published as an Advance Article on the web 26th September 2003

Several new boron compounds containing the 2,4,6-$(CF_3)_3C_6H_2$ (fluoromes = Ar), 2,6-$(CF_3)_2C_6H_3$ (fluoroxyl = Ar′) or 2,4-$(CF_3)_2C_6H_3$ (Ar″) ligands have been synthesised from reactions of ArLi, Ar′Li or Ar″Li with BCl_3, and characterised by ^{19}F and ^{11}B NMR spectroscopy. Chlorine/fluorine exchanges are evident in these reactions. The crystal and molecular structures of Ar_2BF, Ar''_3B, $Ar_2B(OH)$, $Ar'B(OH)_2$ and Mes_2BF (Mes = 2,4,6-$Me_3C_6H_2$) have been determined by single crystal X-ray diffraction. Ar''_3B represents the first example of a compound containing three Ar″ ligands to be structurally characterised. Molecular geometries and GIAO-NMR shifts for several new boron compounds have been calculated at the HF/6-31G* level of theory, and compared with the available experimental results.

Introduction

Although the chemistry of 2,4,6-$(CF_3)_3C_6H_2$ (fluoromes = Ar), 2,6-$(CF_3)_2C_6H_3$ (fluoroxyl = Ar′) and 2,4-$(CF_3)_2C_6H_3$ (Ar″) has been well-developed over the last 15 years,[1–6] little has been published about the ability of these ligands to stabilise group 13 elements. Schluter *et al.* described the syntheses of indium and gallium derivatives containing the 2,4,6-$(CF_3)_3C_6H_2$ (Ar) ligand.[6,7] Bardají *et al.* reported the formation of a thallium derivative, Ar_3Tl.[8] No syntheses of aluminium derivatives of these ligands have been reported to date.

However, the most studied group 13 element involving the ligands Ar, Ar′ or Ar″ is boron. A preliminary conference report mentioned the formation of $ArBCl_2$ **7** and Ar_2BCl **1** from reaction of ArLi with BCl_3, and the occurrence of Cl/F exchange.[2] Ishihara *et al*. explored the arylboronic acid $ArB(OH)_2$ **12** as a catalyst for amidination of carboxylic acids, and the acid $Ar''B(OH)_2$ **21** as a catalyst precursor in the asymmetric allylation of aldehydes with allyltrimethylsilanes.[9,10] Gibson *et al.* reported the preparation of Ar_2BCl **1** from the reaction of ArLi with boron trichloride, and its hydrolysis to give the boronic acid $Ar_2B(OH)$ **2**, as shown in Scheme 1.[11] A lithium complex of type $[LiOBAr_2]$ **3** and a molybdenum complex **4** were synthesised from this acid **2**. The synthesis of Ar_2BN_3 **5** from Ar_2BCl and Me_3SiN_3 was described by Fraenk *et al.*, and an X-ray structure of the partially hydrolysed product, a 1 : 1 $Ar_2BN_3{\cdot}Ar_2B(OH)$ complex **6**, was obtained.[12]

Here we report in detail the separate reactions of ArLi and an Ar′Li/Ar″Li mixture with BCl_3. The numerous boron species formed have been characterised by ^{19}F and ^{11}B NMR solution-state spectroscopy. These reactions clearly involve intriguing fluorine/chlorine exchanges. We show that compound Ar_2BCl **1**, reported as the major product[11,12] from the reaction of ArLi and BCl_3, is in fact the boron–fluorine compound Ar_2BF **8**. This has been confirmed by single crystal X-ray diffraction. The molecular structure of the known[13] dimesitylfluoroborane Mes_2BF **22** (Mes = 2,4,6-$Me_3C_6H_2$) has been similarly ascertained, to compare with that of **8**. The structures of $Ar_2B(OH)$ **2**, Ar''_3B **16** and $Ar'B(OH)_2$ **17** have also been determined by low-temperature X-ray crystallography. In addition, molecular geometries and GIAO-NMR shifts for several boron compounds have been calculated at the HF/6-31G* level of theory, and compared with the experimental results, where available.

Results and discussion

Synthesis and solution-state NMR spectroscopy

Slow addition of ArLi to a $BCl_3{\cdot}OEt_2$ solution in diethyl ether, keeping the boron reagent in excess (Scheme 2), gave rise to a mixture of $ArBCl_2$ **7** and Ar_2BF **8**, identified from their ^{19}F and ^{11}B NMR spectroscopic data (Table 1). Ar_2BF **8** was isolated and fully characterised by X-ray crystallography. In addition, boron trihalide–diethyl etherate adducts were observed in solution ($BFCl_2{\cdot}OEt_2$ **9**, $BF_2Cl{\cdot}OEt_2$ **10** and $BF_3{\cdot}OEt_2$ **11**, Table 1). Their NMR data are very similar to literature results.[14]

When the reaction was carried out by addition of $BCl_3{\cdot}OEt_2$ to excess ArLi, the products observed were $ArBF_2{\cdot}OEt_2$ **13** and Ar_2BF **8** (Scheme 3). ^{19}F and ^{11}B NMR data for **13** are included in Table 1. Adducts **9**–**11** were not detected in this instance.

Fluorine-19 NMR spectroscopy shows for the three compounds **7**, **8** and **13** the characteristic signals of the Ar ligand: a resonance at around −57 ppm for the *ortho*-CF_3 groups, and a singlet at about −64 ppm corresponding to the *para*-CF_3 groups. (Table 1) The couplings in the ^{19}F NMR spectra of a triplet (−56.2 ppm, $^5J_{F-F}$ 15.4 Hz) and a doublet (−57.4 ppm, $^5J_{F-F}$ 14.3 Hz) for $ArBF_2{\cdot}OEt_2$ **13** and Ar_2BF **8**, respectively arise from the fluorines attached to the boron atoms. The latter signal has been confirmed as a doublet by recording the ^{19}F spectrum at two frequencies (188.18 and 376.35 MHz). In both sets of ^{19}F NMR data reported in the literature[11,12] for the incorrectly characterised compound **1**, the two peaks assigned to the *ortho*-CF_3 groups are in fact a doublet, and this compound is really Ar_2BF **8**.

For the diaryl compound **8**, a weak broad multiplet (arising from both spin–spin coupling and the quadrupolar nature of boron) is observed at −9.1 ppm, assigned to the boron-bound fluorine. A similar value of −14.5 ppm is found for the related dimesitylfluoroborane **22**. The ^{19}F signal for the fluorines bound to boron in $ArBF_2{\cdot}OEt_2$ occurs at −145.9 ppm, at significantly lower frequency than those reported for other arylboron difluorides.[15] This difference probably arises from the

† Electronic supplementary information (ESI) available: rotatable 3-D molecular structure diagrams of experimental structures of **2**, **8**, **16**, **17** and **22** and of HF/6-31G* optimised geometries in CHIME format and tables of data for the HF/6-31G* optimized geometries. See http://www.rsc.org/suppdata/dt/b3/b309820f/

DOI: 10.1039/b309820f

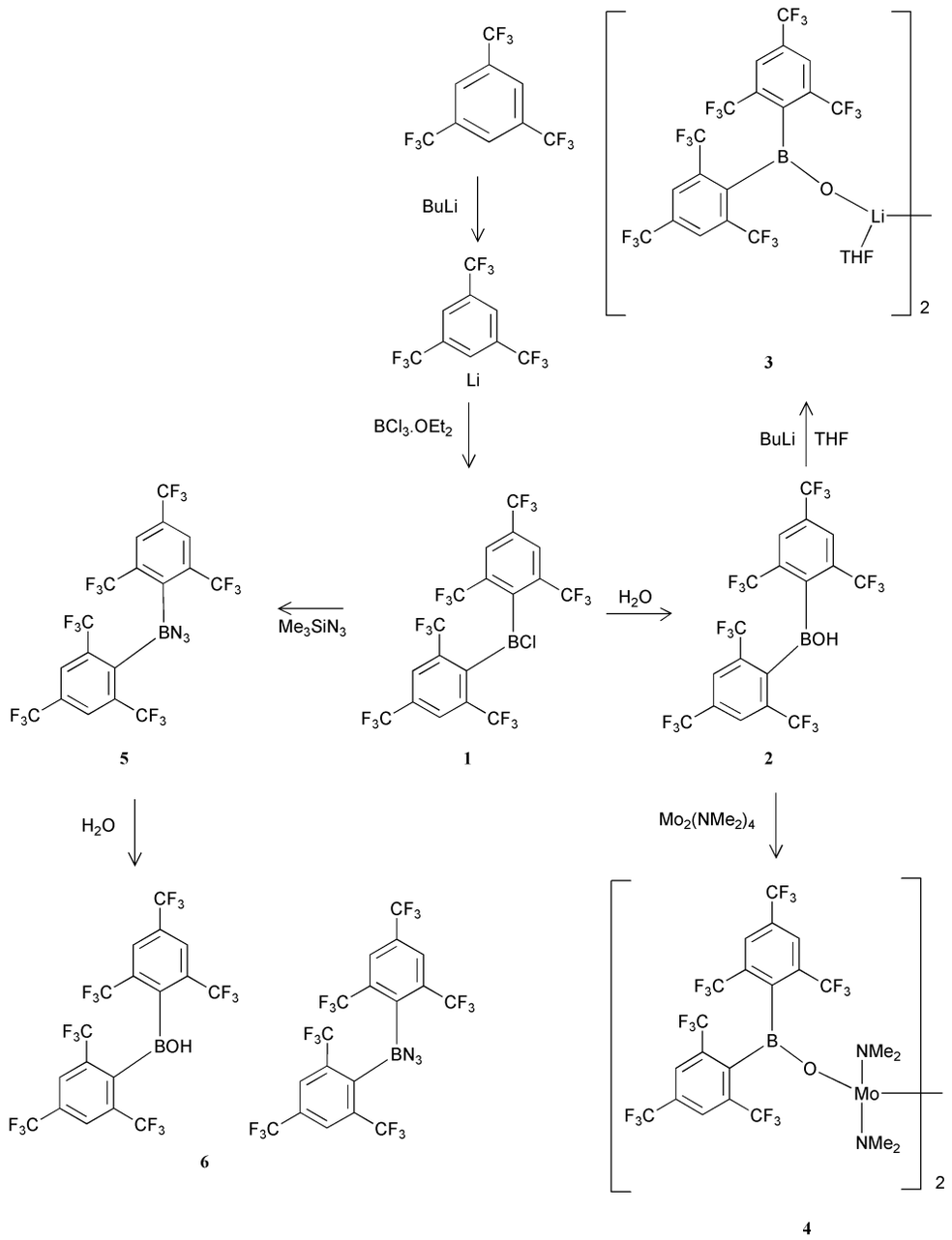

Scheme 1

electron-withdrawing nature of the Ar group, resulting in stronger coordination of Et_2O, as confirmed by the ^{11}B NMR shift of −2.4 ppm. For the similar compound $(C_6F_5)_2BF{\cdot}OEt_2$, a ^{19}F signal at −150.0 ppm for the fluorine bound to boron and an ^{11}B shift of 12.4 ppm have been reported.[16] Very recently, dimethyl[8-(difluoroborolyl)naphthalen-1-yl]amine was found to show clear evidence for formation of an intramolecular 'ate'-complex by donation from N to B of the BF_2 group, with an ^{11}B NMR shift of 10 ppm, and a ^{19}F shift of −149 ppm.[17]

The presence of $ArBF_2{\cdot}OEt_2$ **13** and Ar_2BF **8** (and also the adducts **9**–**11**) can be explained by chlorine/fluorine exchange while the reaction is taking place. This phenomenon has also been observed in the reaction of ArLi with $SiCl_4$.[4,18] The only source of fluorine atoms in the solution is the CF_3 groups in the ArLi compound. No F/Cl exchange between ArH and BCl_3 was found, even after refluxing for 2 h, indicating that exchange does not take place until the aryl group is attached to Li or B. The driving force for this exchange may arise from the relative bond energies. The sum of a C–F and a B–Cl bond energy term (taken from data for the halides[19]) is −929 kJ mol^{-1}, while that for a B–F and a C–Cl bond energy term is −963 kJ mol^{-1}. It is thus energetically favourable for exchange to occur, by −34 kJ mol^{-1}. A similar explanation has been proposed for the observation of F/Cl exchange in Ar, Ar′ and Ar″ silicon derivatives, but not in their germanium or tin analogues.[18] This cannot be the full explanation, however, since similar thermodynamic considerations would apply to a reaction between ArH and BCl_3, where no exchange was detected. It seems probable that a two-stage process is involved. Coordination of the aromatic group to boron brings at least one fluorine from a CF_3 group into close proximity to B, as noted in the crystal structures described below, thus facilitating an intramolecular exchange between F on C and Cl on B. This exchange would generate a species with a $–CF_2Cl$ group in the *ortho*-position of the aromatic moiety, which is not observed in the isolated product. An intermolecular exchange is now possible, however, between Ar_2BCl and the intramolecular exchange product, similar to that seen between $BCl_3{\cdot}OEt_2$ and $BF_3{\cdot}OEt_2$, which is known to be facile,[14] thus allowing the formation of Ar_2BF.

The known[11,12] boronic acid $Ar_2B(OH)$ **2** was obtained by slow hydrolysis of Ar_2BF **8**. The structure of the hydroxy-compound **2** was ascertained by single-crystal X-ray diffrac-

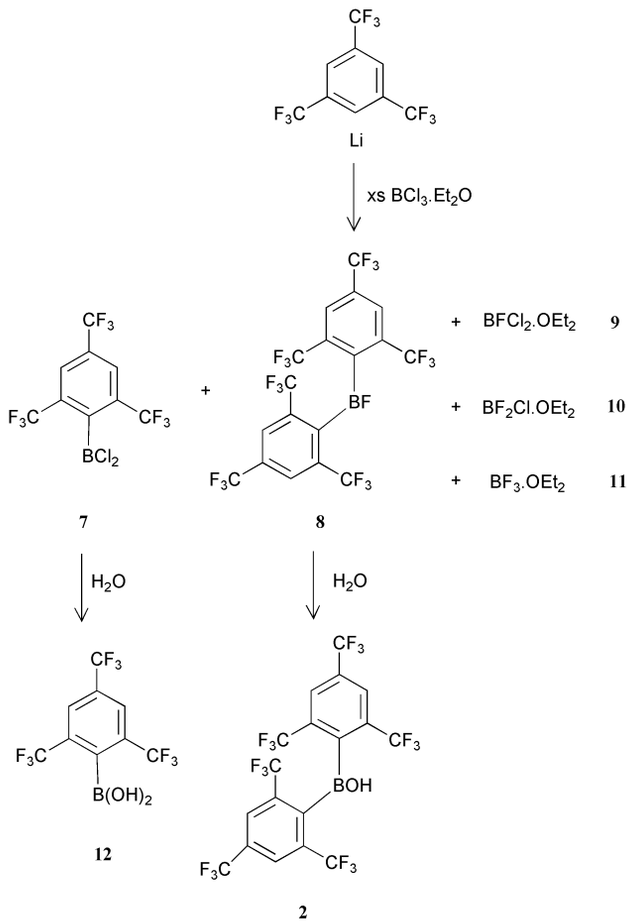

Scheme 2

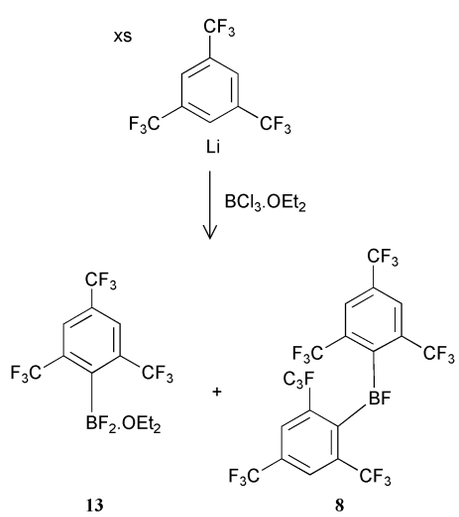

Scheme 3

tion. Facile hydrolysis of $ArBCl_2$ **7** to $ArB(OH)_2$ **12** was observed. ^{19}F and ^{11}B NMR data for these Ar derivatives are included in Table 1. The ^{11}B resonance becomes more shielded on replacing an aryl group with a chlorine atom, and even more so with hydroxy or fluorine substituents, due to increasing π back donation into the vacant orbital on the three-coordinate boron atom.[20]

Reaction of Ar′Li/Ar″Li with BCl_3. A solution containing a mixture of Ar′Li/Ar″Li, obtained from lithiation of 1,3-bis-(trifluoromethyl)benzene Ar′H, was added to excess of a BCl_3 solution in diethyl ether. The ^{19}F and ^{11}B NMR spectra (Table 1) indicated new compounds in solution $Ar'BCl_2$ **14** and Ar'_2BF **15**, identified by comparison with the closely related

Table 1 Experimental and computed fluorine and boron NMR data (ppm) for boron compounds in this study

		$\delta(^{19}F)$	$\delta(^{19}F)$ (calc.)[a,b]	$\delta(^{11}B)$	$\delta(^{11}B)$ (calc.)[a]
Ar_2BOH	**2**	−56.2 (s, 12F, *o*-CF_3), −63.8 (s, 6F, *p*-CF_3)	−79 (*o*-CF_3), −86 (*p*-CF_3)	44.8	40.7
$ArBCl_2$	**7**	−56.4 (s, 6F, *o*-CF_3), −64.0 (s, 3F, *p*-CF_3)	−80 (*o*-CF_3), −85 (*p*-CF_3)	56.8	59.1
Ar_2BF	**8**	−57.4 (d, $^5J_{F-F}$ 14.3 Hz, 12F, *o*-CF_3), −64.0 (s, 6F, *p*-CF_3), −9.1 (m, 1F, BF)	−78 (*o*-CF_3), −86 (*p*-CF_3), −21 (BF)	46.6	43.6
$BCl_3{\cdot}OEt_2$				10.7	16.8
$BFCl_2{\cdot}OEt_2$	**9**	−114.3 (q, $^1J_{B-F}$ 57.6 Hz)	−118	7.9 (d, $^1J_{B-F}$ 58.1 Hz)	10.8
$BF_2Cl{\cdot}OEt_2$	**10**	−128.4 (q, $^1J_{B-F}$ 30.0 Hz)	−134	3.9 (t, $^1J_{B-F}$ 29.0 Hz)	4.4
$BF_3{\cdot}OEt_2$	**11**	−151.2 (s)	−157	0	−0.4
$ArB(OH)_2$	**12**	−56.6 (s, *o*-CF_3), −63.8 (s, *p*-CF_3)	−83 (*o*-CF_3), −85 (*p*-CF_3),	26.0	26.1
$ArBF_2{\cdot}OEt_2$	**13**	−56.2 (t, $^5J_{F-F}$ 15.4 Hz, 6F, *o*-CF_3), −63.8 (s, 3F, *p*-CF_3), −145.9 (m, 2F, BF)	−81 (*o*-CF_3), −85 (*p*-CF_3), −144 (BF)	−2.4	5.3
$Ar'BCl_2$	**14**	−56.9 (s)	−77	57.5	59.3
Ar'_2BF	**15**	−57.2 (d, $^5J_{F-F}$ 14.7 Hz, 6F, CF_3), −12.1 (m, 1F, BF)	−79 (*o*-CF_3), −23 (BF)	46.1	44.1
Ar''_3B	**16**	−56.7 (s, 9F, *o*-CF_3), −63.9 (s, 9F, *p*-CF_3)	−77/−79 [c] (*o*-CF_3), −88/−86 [c] (*p*-CF_3)	73.6	68.1/67.2 [c]
$Ar'B(OH)_2$	**17**	−56.8	−83	26.7	26.4
$Ar'_2BF{\cdot}OH_2$	**18**	−58.8 (d, $^5J_{F-F}$ 22.5 Hz, 6F, CF_3), −189.9 (m, 1F, BF)	−78 (*o*-CF_3), −145 (BF)	5.7	13.0
Ar'_2BOH	**19**	−56.3	−79	45.1	41.2
$Ar''_2BF{\cdot}OEt_2$	**20**	−58.4 (d, $^5J_{F-F}$ 24.6 Hz, 6F, *o*-CF_3), −63.2 (s, 6F, *p*-CF_3), −200.6 (m, 1F, BF)	−81 (*o*-CF_3), −85 (*p*-CF_3), −153 (BF)	8.2	17.3
Mes_2BF	**22**	−14.5	−30	53.0	49.1

[a] At the GIAO-HF/6-31G*//HF/6-31G* level. [b] The computed fluorine shifts are averaged where applicable. [c] From conformation B/conformation A of optimised geometries, respectively.

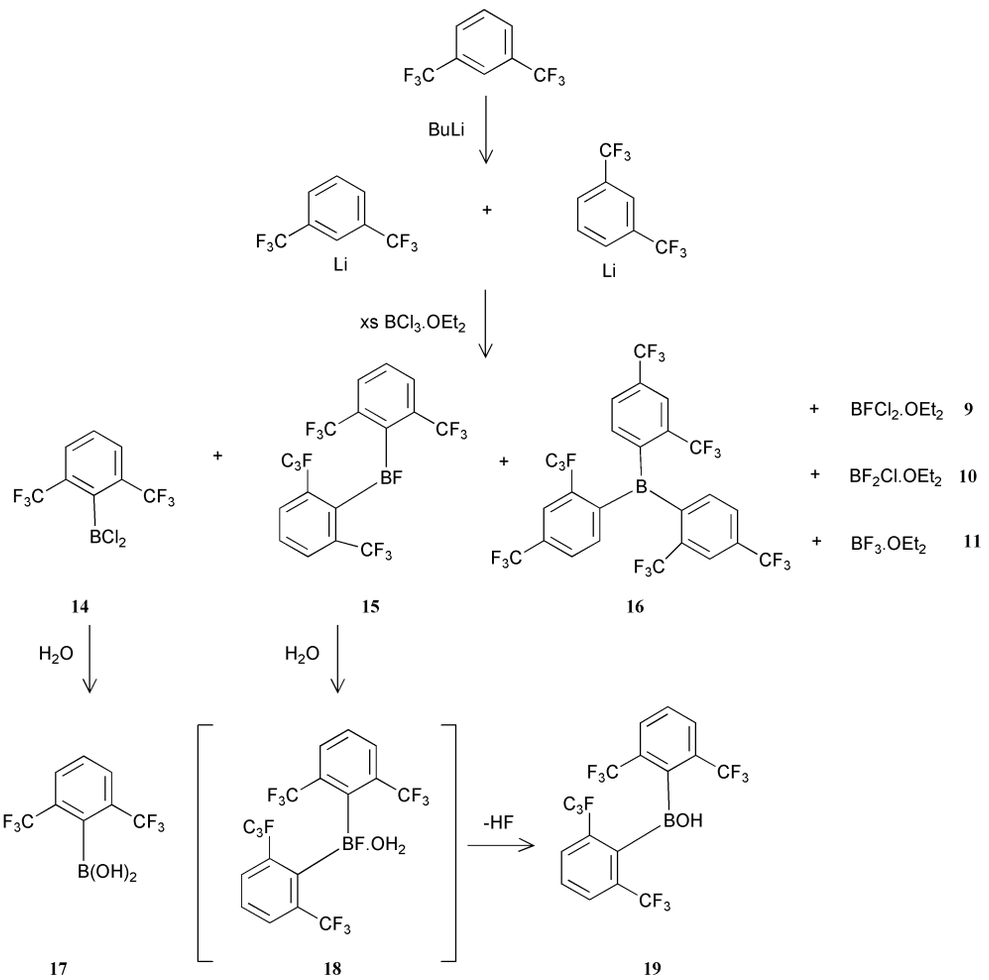

Scheme 4

compounds $ArBCl_2$ **7** and Ar_2BF **8**, respectively. Another new compound Ar''_3B **16** and the known species $BFCl_2{\cdot}OEt_2$ **9**, $BF_2Cl{\cdot}OEt_2$ **10** and $BF_3{\cdot}OEt_2$ **11** (Table 1) were also observed (Scheme 4). The new compounds **14**–**16** were separated by distillation under reduced pressure.

With an excess of Ar′Li/Ar″Li, products **14**, **15** and **16** were again identified in solution, together with the adduct $Ar''_2BF{\cdot}OEt_2$ **20** (Scheme 5, Table 1). The halogen-exchanged derivatives of $BCl_3{\cdot}OEt_2$ were not detected. Hydrolysis of $Ar'BCl_2$ **14** in air gave rise to the formation of $Ar'B(OH)_2$ **17** crystals, which were studied by single-crystal X-ray diffraction. Hydrolysis of Ar'_2BF with H_2O in ether led eventually to $Ar'_2B(OH)$ **19**, via an intermediate **18** retaining a B–F bond according to the NMR spectra. Comparison of the ^{19}F and ^{11}B NMR shifts with theoretical calculations, as discussed below, suggests that this intermediate **18** is probably $Ar'_2BF{\cdot}(OH_2)$, although the anionic species $[Ar'_2BF(OH)]^-$ cannot be entirely discounted on the basis of the results.

The ^{19}F NMR spectrum of Ar''_3B **16** consisted of a singlet at −56.6 ppm (9F, *o*-CF_3) and a singlet at −63.8 ppm (9F, *p*-CF_3) ppm. In order to investigate the rotation of the ring with respect to the B–C bond, ^{19}F NMR spectra of Ar''_3B were recorded in toluene-d_8 between 90 and −80 °C (Fig. 1). No changes were observed until −40 °C, where a new set of signals started to appear. The spectrum at −80 °C showed signals corresponding to two conformations of Ar''_3B (Fig. 2), *i.e.* two singlets at −56.6 and −63.8 ppm, and two singlets at −56.2 and −62.2 ppm, in an overall 5.5 : 1 ratio. At this temperature, by comparison with the variable temperature ^{19}F NMR results for $(2\text{-}CF_3C_6H_5)_3B$,[21] where two signals were only detected at −100 °C in a 0.7 : 1 ratio, it is clear that both conformations **A** and **B** exist in solution, although one of these is dominant. The crystal structure

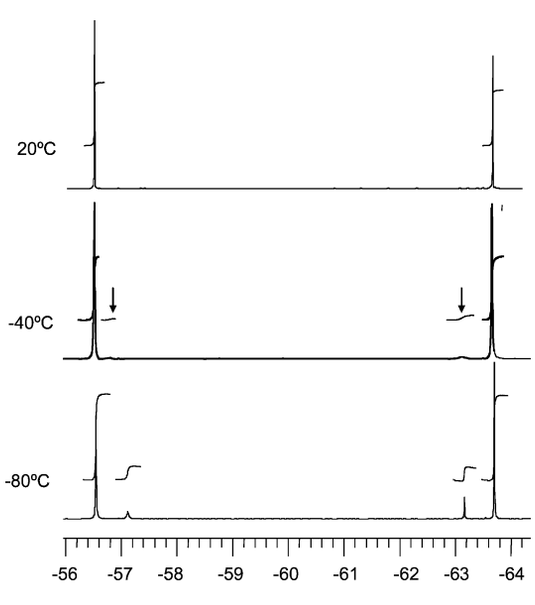

Fig. 1 Variable-temperature ^{19}F NMR spectra of Ar''_3B **16**

determined at −153 °C, discussed in more detail below, shows that the molecule is in conformation **B**, unlike $(2\text{-}CF_3C_6H_4)_3B$ which is in conformation **A** from single-crystal X-ray diffraction at −80 °C.[21] It is thus probable that **B** is the preferred conformation of **16** at −80 °C. Theoretical calculations described below indicate that there is only a very small energy difference between conformations **A** and **B**, with **B** being slightly more stable in each case, thus providing a reasonable

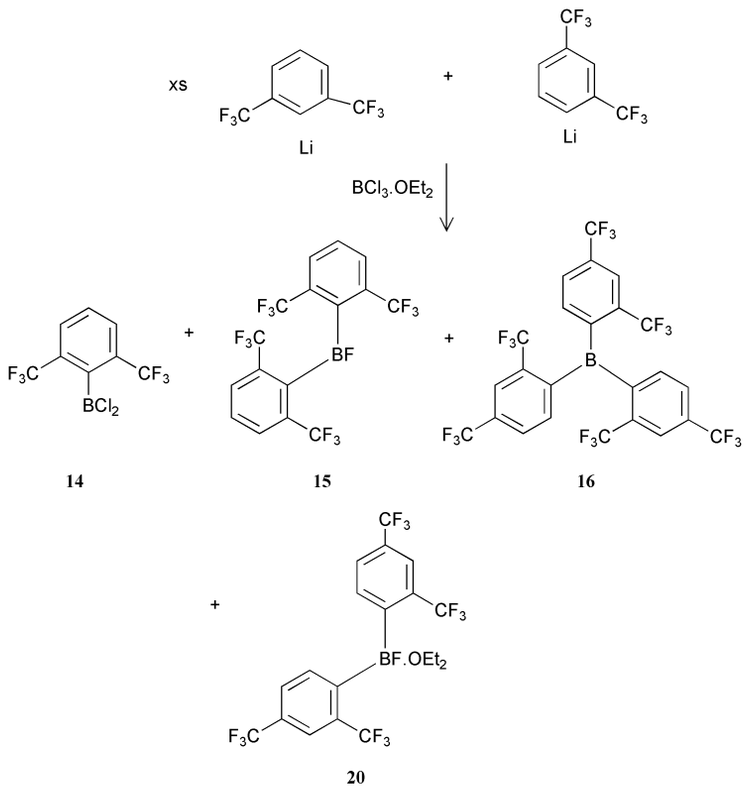

Scheme 5

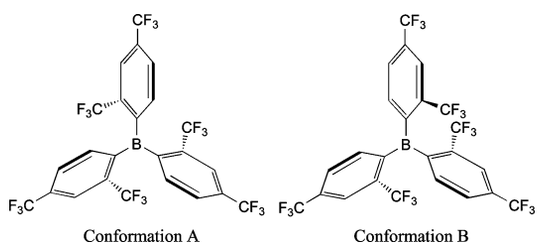

Fig. 2 Different conformations for Ar''_3B **16**

explanation for the low-temperature results. Unfortunately, because of solvent limitations, we were unable to extend these studies to lower temperatures, where further restriction of rotation would be expected, giving rise to two sets of signals in a 2 : 1 ratio from conformation **B**.

X-Ray crystallography

Single-crystal X-ray diffraction studies were carried out at 120 K for compounds $Ar_2B(OH)$ **2**, Ar_2BF **8**, Ar''_3B **16**, and Mes_2BF **22**, and at 100 K for $Ar'B(OH)_2$ **17**. Their molecular structures are illustrated sequentially in Figs. 3–7, respectively. Selected bond distances and angles are listed in Table 2. Rotational disorder was found for the *para*-CF_3 group in Ar_2BF

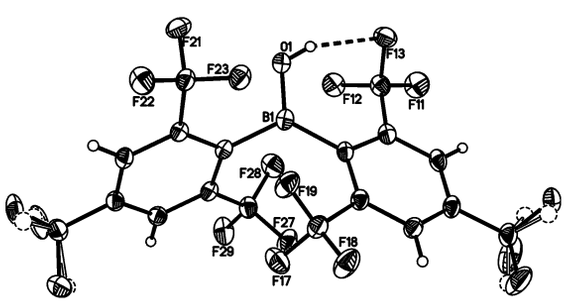

Fig. 3 Molecular geometry of $Ar_2B(OH)$ **2** (atomic displacement ellipsoids in this and the following Figures are drawn at the 50% probability level).

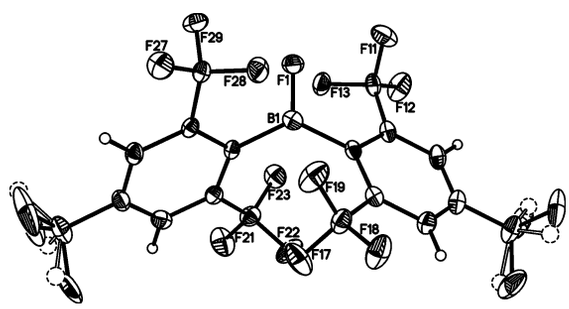

Fig. 4 Molecular geometry of Ar_2BF **8**.

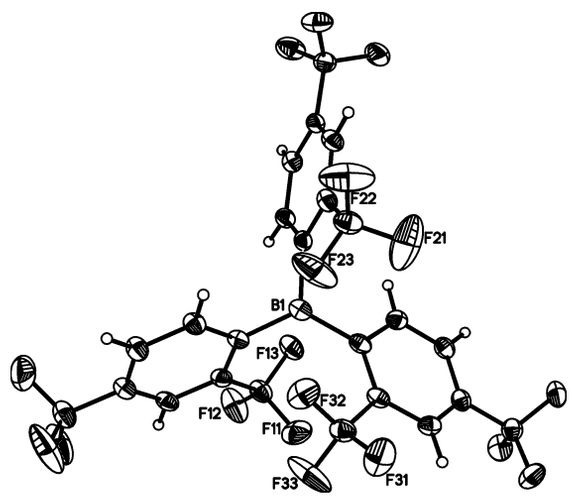

Fig. 5 Molecular geometry of Ar''_3B **16**.

and $Ar_2B(OH)$, as is often observed in compounds containing these ligands.[3,5,18,22]

The structure of $Ar_2B(OH)$ **2** at 200 K has been determined previously by Fraenk *et al* in the 1 : 1 complex of Ar_2BN_3 and Ar_2BOH **6**.[12] Their results are very similar to those obtained at 120 K for **2** in the present work. The O(1)–B(1)–C(21) angle is 112.65(13)° at 120 K, whereas O(1)–B(1)–C(11) is 121.62(14)°.

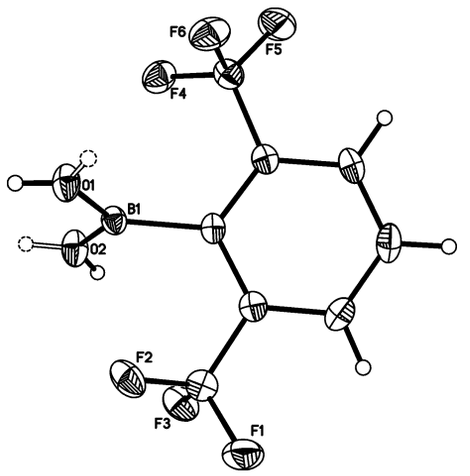

Fig. 6 Molecular geometry of Ar′B(OH)$_2$ **17**. The hydrogens of the –OH groups are disordered over two positions with *ca.* 50% occupancy.

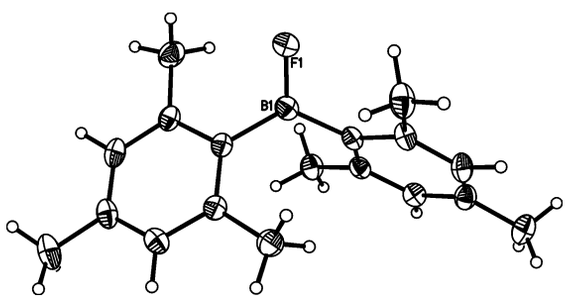

Fig. 7 Molecular geometry of Mes$_2$BF **22**

An intramolecular OH ··· F bridge is found between the hydrogen atom of the OH group and one fluorine atom of a CF_3 group (Fig. 3). The OH distance is 0.78(2) Å, while the H(1) ··· F(13) and H(1) ··· F(12) distances are 2.184(24) and 2.731(23) Å, respectively. The B–C distances in **2** and **8** are similar to those in the 1 : 1 Ar_2BN_3·$Ar_2B(OH)$ complex (1.620(6) and 1.599(7) Å for the two Ar_2B components).[12] C–B–C angles in **2** and **8** (125.73(13) and 128.5(2)°, respectively) are similar to that found in $Mes_2B(OH)$,[23] and larger than the ones of 123.1(2)° in 2,6-$(F_2C_6H_3)_2BCl$[12] and of 123.3(4)° in $(C_6F_5)_2BCl$.[24] This is due to the presence of a bulky group such as CF_3 or CH_3 in the *ortho* position.

Comparison between Ar_2BF **8** (Fig. 4) and Mes_2BF **22** (Fig. 7) shows that the C–B–C angles are similar, reflecting similar steric bulk for Ar and Mes groups. The B–C distances, however, are approximately 0.02 Å longer and the B–F distance is *ca.* 0.03 Å shorter in Ar_2BF than the corresponding bond lengths in Mes_2BF. This is presumably due to reduction of the electron density on the boron atom by the electron-withdrawing Ar groups, thus increasing the π back-donation from the fluorine atom.

A compound containing three Ar″ ligands, Ar″$_3$B **16**, has been structurally characterised for the first time (Fig. 5). Like $(2\text{-}CF_3C_6H_4)_3B$,[21] the triaryl compound Ar″$_3$B exists in a propeller-like geometry, with the three aryl groups twisted out of the plane defined by the three carbons attached to boron. The three rings are twisted by 46.7, 53.7 and 68.9° towards the reference plane made by the three carbons bonded to the boron atom, C(11), C(21) and C(31). These angles are larger than those observed in triphenylborane (28.3°)[25] and $[(3,5\text{-}CF_3)_2C_6H_3]_3B$ (33.3–38.3°),[26] but are similar to those in $(2\text{-}CF_3C_6H_4)_3B$ (40°–55°)[21] and trimesitylborane Mes_3B (40–60°),[27] reflecting the steric size of the *ortho*-substituents. The molecular structure of **16** (Fig. 5) shows that it is in the more stable conformation **B** (Fig. 2), unlike $(2\text{-}CF_3C_6H_4)_3B$ which has conformation **A**. The C–B–C angles in **16** are 117.6(2), 117.0(2) and 124.7(2)°, respectively, for C(11)–B(1)–C(21), C(21)–B(1)–C(31) and

Table 2 Selected bond lengths (Å) and angles (°) for compounds determined by X-ray crystallography

2		**8**		**16**		**17**		**22**	
B(1)–C(11)	1.618(2)	B(1)–C(11)	1.594(4)	B(1)–C(11)	1.582(4)	B(1)–C(1)	1.597(2)	B(1)–C(11)	1.570(2)
B(1)–C(21)	1.608(2)	B(1)–C(21)	1.588(4)	B(1)–C(21)	1.582(4)	B(1)–O(1)	1.355(2)	B(1)–C(21)	1.568(2)
B(1)–O(1)	1.340(2)	B(1)–F(1)	1.313(3)	B(1)–C(31)	1.582(4)	B(1)–O(2)	1.360(2)	B(1)–F(1)	1.339(2)
C(11)–B(1)–C(21)	125.73(13)	C(11)–B(1)–C(21)	128.5(2)	C(11)–B(1)–C(21)	117.6(2)	C(1)–B(1)–O(1)	120.82(14)	C(11)–B(1)–C(21)	125.39(14)
O(1)–B(1)–C(11)	112.65(13)	F(1)–B(1)–C(11)	115.5(2)	C(11)–B(1)–C(31)	124.7(2)	C(1)–B(1)–O(2)	121.03(14)	F(1)–B(1)–C(11)	117.79(14)
O(1)–B(1)–C(21)	121.62(14)	F(1)–B(1)–C(21)	116.0(2)	C(21)–B(1)–C(31)	117.0(2)	O(1)–B(1)–O(2)	118.15(14)	F(1)–B(1)–C(21)	116.82(14)

Table 3 Short B ··· F contacts (Å)

	$Ar_2B(OH)$ **2**	Ar_2BF **8**	Ar''_3B **16**	$Ar'B(OH)_2$ **17**
B–F	2.829–2.914	2.763–2.796	2.800–2.815	2.622–2.634
No. of contacts	4	4	3	2
No. of *ortho*-fluorines	12	12	9	6

C(1)–B(1)–C(31), a distorted trigonal planar geometry of the boron atom. The bond angles at C(11), C(21), and C(31) reveal a significant bending deformation, for example C(12)–C(11)–B(1) 126.7(2)° and C(16)–C(11)–B(1) 116.8(2)°. These significant values are due to close packing between two molecules of **16** in the crystal. There is no such distortion in the reported X-ray structure of $(2\text{-}CF_3C_6H_4)_3B$.[21]

The B–O distances in $Ar'B(OH)_2$ **17** (Fig. 6) are similar to those in the crystal structure of $2,6\text{-}F_2C_6H_3B(OH)_2$, with values of 1.355(2) and 1.360(2) Å in **17**, 1.341(4) and 1.351(4) Å in the difluoro compound,[27] and 1.34(3) and 1.35(3) Å in $3,5\text{-}(CF_3)_2C_6H_3B(OH)_2$, H-bonded in a complex with a carboxylate anion.[28] The angles around boron are close to trigonal in both $Ar'B(OH)_2$, ranging from 118.15(14) to 121.03(14)°, and $2,6\text{-}F_2C_6H_3B(OH)_2$ (118.1(2) to 122.5(2)°),[27] showing that the presence of just one Ar′ group has little effect on the stereochemistry. The B–C distance of 1.597(2) Å in $Ar'B(OH)_2$ **17** is slightly longer than the B–C bond length of 1.578(4) Å reported in $2,6\text{-}F_2C_6H_3B(OH)_2$,[27] and that of 1.56(2) Å in the $3,5\text{-}(CF_3)_2C_6H_3B(OH)_2$ complex.[28] The hydrogens of the –OH groups appear to be disordered over two positions (Fig. 6), with approximately 50% occupancy of each site. Intermolecular hydrogen bonding in the crystal of $Ar'B(OH)_2$ **17** implies that, if a particular hydrogen occupies one such position, this fixes the positions of the three hydroxyl hydrogens forming a repeating unit, as shown by the dotted lines in Fig. 8. While the pattern is not necessarily the same in the next dotted rectangle, there will be a preference for the same orientation, resulting from electrostatics, and giving a symmetrical repeating unit. The O(1) ··· H ··· O(1′), O(2) ··· H ··· O(2′) and O(1) ··· H ··· O(2) (intermolecular) distances are 2.7508(25), 2.7532(25) and 2.6801(16) Å, respectively. Similar hydrogen bonding has been reported for the complex containing the boronic acid $3,5\text{-}(CF_3)_2C_6H_3B(OH)_2$ and a carboxylate anion, with O ··· H ··· O distances of 2.67(2) and 2.64(2) Å.[28]

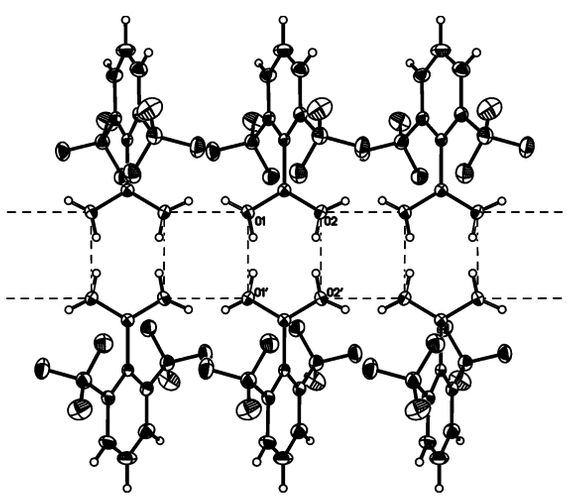

Fig. 8 Repeating pattern *via* hydrogen bonds in crystal of $Ar'B(OH)_2$ **17**

As often described for compounds containing Ar, Ar′ or Ar″ groups,[18,21,22] short contacts between the central atom and some fluorine atoms of the *o*-CF_3 substituents are apparent (Table 3). These compare well with B ··· F contact distances of 2.845(3), 2.816(4) and 2.763(3) Å in $(2\text{-}CF_3C_6H_4)_3B$, even with different conformations of the compounds.[21] The number of contacts depends on the number of trifluoromethyl groups in the *ortho* position. B ··· F contacts are shorter in compounds containing only one aryl ring (Table 3). In $Ar_2B(OH)$ the range of values is somewhat broader, probably because of the F ··· H interaction mentioned above.

Computations

A series of *ab initio* calculations has been performed to provide optimised gas-phase structures and NMR shift data for the boron compounds made here. Use of the computationally intensive MP2/6-31G* level of theory gave excellent agreements between observed and optimised geometries for Mes_2BF (see Table S1, ESI† for details). Removal of the *para*-methyl group did not significantly affect the geometry around the boron atom or the calculated boron shifts. The lower level of theory, HF/6-31G*, gave reasonable agreements between observed and computational data for Mes_2BF. Since there is little justification in using the MP2/6-31G* level of theory here, calculations were carried out at the HF/6-31G* level of theory for the compounds described. Selected parameters for the optimised and experimental geometries of the compounds structurally characterised in this work are also listed in the ESI. The agreement between computed and optimised geometries is very good. As shown from X-ray crystallography, short B ··· F contacts are found. The optimised geometry of $Ar'B(OH)_2$ also shows the presence of an intramolecular F ··· H bridge.

Both conformations (**A** and **B**) of Ar''_3B were optimised at HF/6-31G*, with **B** found to be lower in energy than **A** by *ca.* 4 kJ mol^{-1}. This energy difference is substantially less than 15.5 kJ mol^{-1} reported[21] for the closely related $(2\text{-}CF_3C_6H_4)_3B$ using the AM1 level of theory. The latter borane – a model for Ar''_3B – was computed at the HF/6-31G* level of theory here to give more realistic energy values. Conformation **B** is 2 kJ mol^{-1} lower in energy than **A** in $(2\text{-}CF_3C_6H_4)_3B$ and the rotational barrier between **A** and **B** is 28.9 kJ mol^{-1} with respect to **B**. The rotational barrier between the two enantiomers of **B** is 16.8 kJ mol^{-1}. All these calculated values at the *ab initio* level are in good agreement with the observed ^{19}F NMR data at low temperatures for $(2\text{-}CF_3C_6H_4)_3B$ and Ar''_3B. It is therefore not surprising to find either conformation (**A** or **B**) in the solid-state for $(2\text{-}CF_3C_6H_4)_3B$ and Ar''_3B, considering the very similar energies computed for both conformations.

Since good agreement is found between computed and experimental geometries, geometries for compounds not structurally determined in this work were also optimised at the HF/6-31G* level of theory. The boron environments in optimised geometries for $ArB(OH)_2$, Ar'_2BF and Ar'_2BOH are virtually identical to those in $Ar'B(OH)_2$, Ar_2BF and Ar_2BOH, respectively, showing the *para*-CF_3 group to have little effect on the environment surrounding the boron atom. The neutral chlorides, $ArBCl_2$ and $Ar'BCl_2$, have similar parameters to those found in $ArB(OH)_2$ and $Ar'B(OH)_2$.

Selected parameters from optimised geometries of the adducts, $ArBF_2{\cdot}OEt_2$, $Ar'_2BF{\cdot}OH_2$, $Ar''_2BF{\cdot}OEt_2$ and $BF_xCl_{3-x}{\cdot}OEt_2$ are shown in the ESI.† The adducts all have four-coordinate boron with similar boron environments. There are only two reported examples of arylborane ether adducts structurally characteried, namely $Ph_3B{\cdot}THF$[29] and $Ph_2BCl{\cdot}THF$.[30] Since they are four-coordinate boron compounds, the accuracy of the HF/6-31G* level of theory was examined by comparing the optimised geometry with the X-ray data for $Ph_2BCl{\cdot}THF$. It is clear from the results that the agreement is poor with respect

to the B–O bond length. It is known that the geometries of boron adducts in the gas phase differ considerably from geometries in the solid state, particularly for the bond distances between the boron atom and the Lewis base.[31] The optimised geometries for the adducts made here are therefore expected in the gas-phase and in solution. A different level of theory such as the self-consistent reaction field would be needed for probable solid-state geometries of these adducts.[32] Reported optimised geometries of $BF_3{\cdot}OMe_2$ and $BCl_3{\cdot}OMe_2$ at *ab initio* levels are in good agreement with $BF_3{\cdot}OEt_2$ and $BCl_3{\cdot}OEt_2$ geometries here.[33] The B–O bond distances shorten on going from $BF_3{\cdot}OEt_2$, $BF_2Cl{\cdot}OEt_2$, $BFCl_2{\cdot}OEt_2$ to $BCl_3{\cdot}OEt_2$ as expected from the ligand close-packing theory.[34] Fig. 9 shows an optimised geometry for the adduct $ArBF_2{\cdot}OEt_2$ at the HF/6-31G* level of theory.

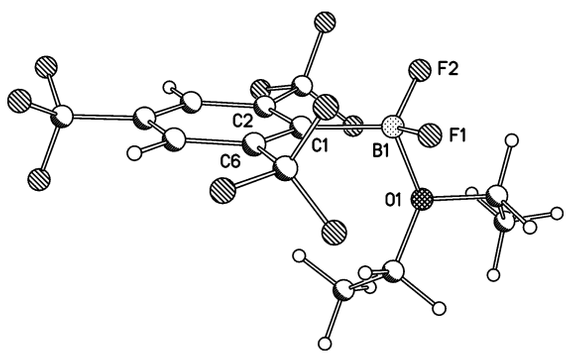

Fig. 9 Optimised molecular geometry for the adduct $ArBF_2{\cdot}OEt_2$ **13**.

Computed boron and fluorine NMR shifts generated from the optimized geometries for all compounds synthesised here are listed in Table 1. These values are in acceptable agreement with observed shifts, apart from the B–F fluorine shifts for $Ar'_2BF{\cdot}OH_2$ and $Ar''_2BF{\cdot}OEt_2$. A related derivative $(C_6F_5)_2BF{\cdot}OEt_2$ was subjected to computations, in order to see whether the presence of two aryl groups in an adduct would give poor computed ^{19}F shifts. The calculated shifts were −149 (*o*-CF), −154 (BF), −170 (*p*-CF), −186 ppm (*m*-CF) for ^{19}F and 13.0 ppm for ^{11}B, in good agreement with reported data (−134 (*o*-CF), −150 (BF), −155 (*p*-CF), −163 ppm (*m*-CF) for ^{19}F and 12.4 ppm for ^{11}B).[16] Selected parameters for the optimized geometry of $(C_6F_5)_2BF{\cdot}OEt_2$ are also shown in Table S2 (ESI†). Possible alternatives to $Ar'_2BF{\cdot}OH_2$ and $Ar''_2BF{\cdot}OEt_2$ such as Ar'_2BFOH^- anion and $Ar''BClF{\cdot}OEt_2$, respectively, were also examined by computations, and neither gave significantly better agreement in the NMR shifts. At present, identification of $Ar'_2BF{\cdot}OH_2$ and $Ar''_2BF{\cdot}OEt_2$, with the four groups attached to boron in these adducts collectively very bulky, is tentative.

Experimental

All manipulations, including NMR sample preparation, were carried out either under an inert atmosphere of dry nitrogen or *in vacuo*, using standard Schlenk procedures or in a glovebox. Chemicals of the best available commercial grades were used, in general without further purification. ^{19}F NMR spectra were recorded on Varian Mercury 200, Varian VXR 400, or Varian Inova 500 Fourier-transform spectrometers at 188.18, 376.35, and 470.26 MHz, respectively. ^{11}B NMR spectra were recorded on the Varian Mercury 300 or Varian Inova 500 spectrometers at 96.22 and 160.35 MHz, respectively. ^1H and ^{13}C NMR spectra were recorded on the Varian VXR 400 instrument at 400 and 100.57 MHz, respectively, for Ar''_3B only. Ambient-temperature NMR spectra were obtained using $CDCl_3$ as solvent for isolated compounds; the NMR spectra of reaction mixtures were recorded in the solvent(s) used for the reaction, with a little $CDCl_3$ added to provide the deuterium lock. Chemical shifts were measured relative to external $CFCl_3$ (^{19}F) or $BF_3{\cdot}Et_2O$ (^{11}B), with the higher frequency direction taken as positive. Mass spectra for isolated samples were recorded on a VG Micromass 7070E instrument under EI conditions at 70 eV and for impure samples on a Fisons VG Trio 1000 mass spectrometer coupled directly to a Hewlett Packard 5890 Series II gas chromatograph (Column: HP-1; 25 m; 0.25 mm I.D.; 0.32 μm film thickness). Mes_2BF was synthesised according to the literature.[13]

Synthesis of $ArBCl_2$ 7 and Ar_2BF 8. A solution of ArLi was prepared by adding BuLi (28 ml, 1.6 M in hexanes, 44.8 mmol) dropwise to a stirred solution of ArH (12.8 g, 45.4 mmol) in 100 ml of Et_2O at −78 °C and leaving the mixture to warm to room temperature for 5 h. Fluorine NMR spectroscopy on a sample of the solution revealed two peaks corresponding to ArLi at −62.6 (*o*-CF_3) and −62.8 (*p*-CF_3) ppm, and a small peak at −63.7 ppm assigned to ArH. To the yellow ArLi solution was added dropwise *via* cannula a BCl_3 solution (100 ml, 1 M in heptane, 100 mmol) in diethyl ether (50 ml) at −78 °C. The reaction mixture was allowed to warm to room temperature for 6 h with stirring, leaving a yellow solution and a white precipitate. The solution was then filtered and solvents were removed *in vacuo*, leaving a yellow oil and a white solid. This mixture was vacuum distilled at 60 °C/0.05 Torr to give a fraction containing $ArBCl_2$ **7** (0.8 g, 5% yield) and the adducts $BF_xCl_{3-x}{\cdot}OEt_2$ (2.6 g). The residue was then sublimed at 95 °C under vacuum to give a white solid identified as Ar_2BF **8** (3.2 g, 24% yield). Crystals of Ar_2BF were obtained by recrystallisation from dichloromethane.

$ArBCl_2$: ^1H NMR: 8.07 (s) ppm. ^{13}C NMR: 134.6 (q, $^2J_{C-F}$ 35.1 Hz), 132.7 (q, $^2J_{C-F}$ 32.7 Hz), 125.6 (septet, $^3J_{C-F}$ 3.0 Hz, CH), 123.0 (q, $^1J_{C-F}$ 273.8 Hz), 122.7 (q, $^1J_{C-F}$ 274.2 Hz) ppm. GC-MS: *m*/*z* 362 (M, calc. for $C_9H_2F_9BCl_2$: 362, with expected pattern at 361–364 from ^{10}B, ^{11}B, ^{35}Cl and ^{37}Cl isotopes), 327 (M − Cl).

Ar_2BF: ^1H NMR: 8.17 (s) ppm. ^{13}C NMR: 137.2 (q, $^2J_{C-F}$ 38.0 Hz), 134.5 (q, $^2J_{C-F}$ 34.4 Hz), 134.1 (CB), 126.6 (septet, $^3J_{C-F}$ 3.0 Hz, CH), 122.8 (q, $^1J_{C-F}$ 275.2 Hz), 122.3 (q, $^1J_{C-F}$ 273.0 Hz) ppm. EI-MS: *m*/*z* – (M, calc. for $C_{18}H_4F_{19}B$ 592), 573 (M–F, pattern at 572–574 from ^{10}B, ^{11}B and ^{13}C), 505 (M − CF_4 + H).

Synthesis of $Ar'BCl_2$ 14, Ar'_2BF 15 and Ar''_3B 16. A solution of Ar′/Ar″Li was generated by adding BuLi (28 ml, 1.6 M in hexanes, 44.8 mmol) dropwise to a stirred solution of Ar′H (10.5 g, 49.1 mmol) in 100 ml of Et_2O at −78 °C and left to warm to room temperature for 4 h. Fluorine NMR spectroscopy on a sample of the solution revealed two peaks corresponding to Ar″Li at −61.9 (*o*-CF_3) and −62.8 (*p*-CF_3) ppm, a peak corresponding to Ar′Li at −62.1 ppm and a small peak at −63.7 ppm assigned to Ar′H. The ^{19}F peak integrals indicate the solution to contain a Ar′Li : Ar″Li ratio of 3 : 4. To the dark brown solution of Ar′/Ar″Li was added dropwise *via* cannula, a solution of BCl_3 (100 ml, 1 M in heptane, 100 mmol) in Et_2O (50 ml) at −78 °C. The reaction mixture was allowed to warm to room temperature for 3 h, leaving a brown solution and a white precipitate. The solution was filtered and the solvents removed *in vacuo*, leaving a brown oil, which was distilled under reduced pressure (0.05 Torr). A fraction containing $Ar'BCl_2$ **14** (1.8 g, 14% yield) and the adducts $BF_xCl_{3-x}{\cdot}OEt_2$ (3.2 g) was collected at 48 °C. A second colourless fraction was collected at 92 °C and identified as Ar'_2BF **15** (0.5 g, 5% yield). The white solid remained in the flask was sublimed under vacuum at 120 °C, affording Ar''_3B **16** as a white crystalline solid (1.6 g, 17% yield). A crystal of Ar''_3B suitable for X-ray study was obtained by recrystallization from hexane.

$Ar'BCl_2$: ^1H NMR: 7.88 (d, J_{HH} 7.8 Hz, 2H), 7.73 (t, J_{HH} 7.8 Hz, 1H) ppm. ^{13}C NMR: 132.7 (q, $^2J_{C-F}$ 33.0 Hz), 130.8 (s, CH), 129.5 (q, $^3J_{C-F}$ 2.9 Hz, CH), 123.7 (q, $^1J_{C-F}$ 272.7 Hz) ppm.

Table 4 Crystal data and structure refinement parameters

	$Ar'_2B(OH)$ **2**	Ar_2BF **8**	Ar''_3B **16**	$Ar'B(OH)_2$ **17**	Mes_2BF **22**
Empirical formula	$C_{18}H_5BF_{18}O$	$C_{18}H_4BF_{19}$	$C_{24}H_9BF_{18}$	$C_8H_5BF_6O_2$	$C_{18}H_{22}BF$
M_r	590.03	592.02	650.12	257.93	268.17
Crystal system	Triclinic	Monoclinic	Triclinic	Orthorhombic	Monoclinic
Space group	$P\bar{1}$	$P2_1/n$	$P\bar{1}$	$P2_12_12$	$P2_1/c$
Crystal size/mm	0.38 × 0.24 × 0.18	0.20 × 0.20 × 0.05	0.50 × 0.20 × 0.10	0.43 × 0.20 × 0.10	0.30 × 0.22 × 0.20
T/K	120(2)	120(2)	120(2)	100(2)	120(2)
a/Å	9.1587(3)	8.9564(6)	10.1795(7)	14.0859(14)	8.2080(5)
b/Å	10.1298(3)	9.4751(6)	11.0533(8)	14.4620(14)	7.8003(5)
c/Å	12.5200(4)	23.6514(15)	11.4719(8)	5.0028(5)	24.0891(16)
α/°	112.5700(10)	90	94.9440(10)	90	90
β/°	99.9530(10)	98.494(1)	108.3620(10)	90	90.3380(10)
γ/°	102.5760(10)	90	94.5490(10)	90	90
V/Å^3	1003.60(5)	1985.1(2)	1212.75(15)	1019.12(17)	1542.27(17)
Z	2	4	2	4	4
D_c/g cm^{-3}	1.953	1.981	1.78	1.681	1.155
μ/mm^{-1}	0.234	0.241	0.200	0.187	0.072
R_{int}	0.0274	0.0736	0.0365	0.0283	0.0388
Observed data [$I > 2\sigma(I)$]	3844	2748	3840	2209	2719
R_1 index [$I > 2\sigma(I)$]	0.0359	0.0469	0.0528	0.0305	0.0528
R_1 index (all data)	0.0447	0.0982	0.0741	0.0333	0.0795
wR_2 index [$I > 2\sigma(I)$]	0.0914	0.0924	0.1255	0.0717	0.1274
wR_2 index (all data)	0.0981	0.1113	0.1362	0.0735	0.1418
Goodness of fit (S)	1.022	1.026	1.057	1.122	1.025
No. of variables	386	381	388	169	269

GC-MS: *m*/*z* 294 (M, calc. for $C_8H_3F_6BCl_2$ 294), 259 (M − Cl, isotope pattern at 258–261).

Ar'_2BF: ^{1}H NMR: 7.97 (d, J_{HH} 8.0 Hz, 2H), 7.78 (t, J_{HH} 8.0 Hz, 1H) ppm. ^{13}C NMR: 133.7 (q, $^2J_{C-F}$ 34.5 Hz), 131.5 (s, CH), 129.2 (q, $^3J_{C-F}$ 3.0 Hz, CH), 123.3 (q, $^1J_{C-F}$ 275.2 Hz) ppm. EI-MS: *m*/*z* 456 (M, calc. for $C_{16}H_6F_{13}B$ 456), 369 (M–CF_4 + H, isotope pattern at 368–370).

Ar''_3B: ^{1}H NMR: 8.00 (s, 1H), 7.80 (d, J_{HH} 7.6 Hz, 1H), 7.41 (d, J_{HH} 7.6 Hz, 1H) ppm. ^{13}C NMR: 143.7 (CB), 135.4 (s, CH), 133.6 (q, $^2J_{C-F}$ 34.3 Hz), 133.5 (q, $^2J_{C-F}$ 33.7 Hz), 127.3 (q, $^3J_{C-F}$ 3.6 Hz, CH) 123.1 (septet, $^3J_{C-F}$ 3.0 Hz, CH), 123.1 (q, $^1J_{C-F}$ 274.5 Hz), 122.9 (q, $^1J_{C-F}$ 273.0 Hz) ppm. EI-MS: *m*/*z* 650 (M, calc. for $C_{24}H_9F_{18}B$ 650), 631 (M − F, isotope pattern at 630–632), 436 (M − Ar″ − H).

Synthesis of Ar_2BOH 2. Distilled water (5 ml) was added dropwise to a stirred solution of Ar_2BF (0.5g, 0.85 mmol) in ether (30 ml). The ether layer was separated and dried *in vacuo* to yield a white solid Ar_2BOH **2** (0.4 g, 80%). This solid was recrystallized from dichloromethane to yield crystals suitable for X-ray crystallography.

Ar_2BOH: ^{1}H NMR: 8.15 (CH, 4H, s), 7.87 (OH, 1H, s) ppm. ^{13}C NMR: 138.5 (CB), 136.8 (q, $^2J_{C-F}$ 35.2 Hz), 133.4 (q, $^2J_{C-F}$ 34.4 Hz), 126.6 (septet, $^3J_{C-F}$ 3.0 Hz, CH), 123.0 (q, $^1J_{C-F}$ 275.2 Hz), 122.4 (q, $^1J_{C-F}$ 273.1 Hz) ppm.

Synthesis of Ar'_2BOH 19. The method for the synthesis of Ar_2BOH was also used to convert Ar'_2BF into Ar'_2BOH in a similar yield. Fluorine and boron NMR spectra on an aliquot of the ether layer after 30 min stirring revealed an intermediate, presumed to be $Ar'_2BF{\cdot}OH_2$. The NMR data for the intermediate were recorded from a $CDCl_3$ solution of Ar'_2BF with a drop of water and two drops of ether added.

Ar'_2BOH: ^{1}H NMR: 7.94 (d, J_{HH} 8.0 Hz, 2H), 7.69 (t, J_{HH} 8.0 Hz, 1H) ppm. ^{13}C NMR 132.5 (q, $^2J_{C-F}$ 34.2 Hz), 130.5 (s, CH), 129.6 (q, $^3J_{C-F}$ 3.7 Hz, CH), 123.6 (q, $^1J_{C-F}$ 275.2 Hz) ppm.

Syntheses of $Ar'B(OH)_2$ 17 and $ArB(OH)_2$ 12. A portion of the distilled fraction containing $Ar'BCl_2$ and the adducts $BF_xCl_{3-x}{\cdot}OEt_2$ in ether was left exposed to air. After two days, white crystals were formed and identified by X-ray crystallography as $Ar'B(OH)_2$. A solid was obtained from slow exposure to air of a sample of $ArBCl_2$ and the adducts $BF_xCl_{3-x}{\cdot}OEt_2$, and tentatively identified by NMR as $ArB(OH)_2$.

Reaction of BCl_3 with excess ArLi. A solution of ArLi was made by adding BuLi (28 ml, 1.6 M in hexanes, 44.8 mmol) dropwise to a stirred solution of ArH (12.8 g, 45.4 mmol) in 100 ml of Et_2O at −78 °C and left to warm to room temperature overnight. The light brown solution was slowly treated with BCl_3 (6 ml, 1 M in heptane, 6 mmol) at −78 °C, and left to warm to room temperature for 1 h. Fluorine and boron NMR spectra were obtained from a sample of the reaction mixture which showed $ArBF_2{\cdot}OEt_2$ to be the major product. Ar_2BF and a substantial amount of unreacted ArLi were also present. To the reaction mixture was then added a further 6 ml of BCl_3 (1 M in heptane, 6 mmol) at −78 °C. After warming the mixture to room temperature, ^{19}F and ^{11}B NMR data on an aliquot of the solution gave Ar_2BF as the major component and $ArBF_2{\cdot}OEt_2$ as the only other significant compound. On removing the ether and heptane *in vacuo*, the residue contained a yellow oil and a white solid. NMR data on the yellow oil revealed Ar_2BF but no $ArBF_2{\cdot}OEt_2$. It is presumed the latter adduct dissociated into $ArBF_2$ and Et_2O on removing the ether *in vacuo*. Vacuum sublimation of the residue at 93 °C gave a white solid identified as Ar_2BF (3.3 g, 46% yield).

Reaction of BCl_3 with excess Ar′Li. A solution of Ar′/Ar″Li was generated by adding BuLi (28 ml, 1.6 M in hexanes, 44.8 mmol) dropwise to a stirred solution of Ar′H (10.5 g, 49.1 mmol) in 100 ml of Et_2O at −78 °C and left to warm to room temperature overnight. The brown solution was slowly treated with BCl_3 (6 ml, 1 M in heptane, 6 mmol) at −78 °C and left to warm to room temperature for 1 h. Fluorine and boron NMR spectra obtained from a sample of the reaction mixture revealed Ar''_3B to be the major product. $Ar''_2BF{\cdot}OEt_2$ and unreacted Ar′Li were also present. The reaction mixture was then treated with a further 6 ml of BCl_3 (1 M in heptane, 6 mmol) at −78 °C. After warming the mixture to room temperature, ^{19}F and ^{11}B NMR data on an aliquot of the solution gave Ar''_3B and Ar'_2BF as the major components. $Ar''_2BF{\cdot}OEt_2$ and $Ar'BCl_2$ were also observed. On removing the ether and heptane *in vacuo*, the residue contained a yellow oil and a white solid. NMR data on the yellow oil revealed only Ar''_3B and Ar'_2BF. The fates of $Ar''_2BF{\cdot}OEt_2$ and $Ar'BCl_2$ are not clear.

Crystallography. Single crystal structure determinations were carried out from data collected at 100 or 120 K, using graphite monochromated Mo-Kα radiation (λ = 0.71073 Å) on a Bruker

SMART-CCD detector diffractometer equipped with a Cryostream N_2 flow cooling device.[35] In each case, series of narrow ω-scans (0.3°) were performed at several ϕ-settings in such a way as to cover a sphere of data to a maximum resolution between 0.70 and 0.77 Å. Cell parameters were determined and refined using the SMART software,[36] and raw frame data were integrated using the SAINT program.[37] The structures were solved using direct methods and refined by full-matrix least squares on F^2 using SHELXTL.[38] Relevant parameters for data collection and structure solution are given in Table 4

CCDC reference numbers 217588–217592.

See http://www.rsc.org/suppdata/dt/b3/b309820f/ for crystallographic data in CIF or other electronic format.

Computational methods. All *ab initio* computations were carried out with the Gaussian 98 package.[39] All geometries discussed here were optimised at the HF/6-31G* level with no symmetry constraints. Frequency calculations were computed on these optimised geometries at the HF/6-31G* level for imaginary frequencies; none was found for geometries where the *para* CF_3 group is absent. Theoretical ^{11}B chemical shifts at the GIAO-HF/6-31G*//HF/6-31G* level have been referenced to B_2H_6 (16.6 ppm)[40] and converted to the usual $BF_3{\cdot}OEt_2$ scale: $\delta(^{11}B) = 123.4 - \sigma(^{11}B)$. For Mes_2BF, the HF/6-31G* optimised geometry in Table 4 was then optimised at the MP2/6-31G* level of theory, and the ^{11}B shift of 55.4 ppm was computed from the MP2 optimised geometry at the GIAO-B3LYP/6-311G* level of theory with the scale: $\delta(^{11}B) = 102.84 - \sigma(^{11}B)$. Unlike the excellent agreements between observed and computed ^{11}B NMR shifts of fluoroboranes, computed ^{19}F NMR shifts have not been shown to be as accurate.[41,42] Here, calculated ^{19}F chemical shifts at the GIAO-HF/6-31G*//HF/6-31G* level have been referenced to HF and converted to the usual $CFCl_3$ scale: $\delta(^{19}F) = (237.7 - \sigma(^{19}F))/0.911$. Computed NMR shifts (GIAO-HF/6-31G*//HF/6-31G*) for $Ar''BFCl{\cdot}OEt_2$: ^{11}B 12.0 ppm; ^{19}F −84 (*o*-CF_3), −86 (*p*-CF_3), −135 (BF) ppm; for Ar'_2BFOH^-: ^{11}B 3.8 ppm; ^{19}F −78 (CF_3), −158 (BF) ppm; for dimethyl[8-(difluoroborolyl)naphthalen-1-yl]amine: ^{11}B 9.9 ppm; ^{19}F −146 ppm.[17] Cartesian coordinates for the optimised geometries obtained are available in the ESI.†

Acknowledgements

We thank the EPSRC for the award of studentships (to S. M. C., C. D. E., H. P. G., and A. L. T.), for an Advanced Research Fellowship (to M. A. F.), and C. F. Heffernan, A. M. Kenwright and I. P. McKeag for assistance in recording some of the NMR spectra.

References

1 G. E. Carr, R. D. Chambers, T. F. Holmes and D. G. Parker, *J. Organomet. Chem.*, 1987, **325**, 13; M. Scholz, H. W. Roesky, D. Stalke, K. Keller and F. T. Edelmann, *J. Organomet. Chem.*, 1989, **366**, 73; H. Grutzmacher, H. Pritzkow and F. T. Edelmann, *Organometallics*, 1991, **10**, 23; S. Brooker, J. Buijink and F. T. Edelmann, *Organometallics*, 1991, **10**, 25; M. Abe, K. Toyota and M. Yoshifuji, *Chem Lett.*, 1992, **12**, 259; K. B. Dillon and H. P. Goodwin, *J. Organomet. Chem.*, 1992, **429**, 169; K. B. Dillon and H. P. Goodwin, *J. Organomet. Chem.*, 1994, **469**, 125; F. T. Edelmann, *Comments Inorg. Chem.*, 1992, **12**, 259; M. Belay and F. T. Edelmann, *J. Organomet. Chem.*, 1994, **479**, C21; J.-T. Alhemann, H. W. Roesky, M. Noltemeyer, H.-G. Schmidt, L. N. Markovsky and Y. G. Shermolovich, *J. Fluorine Chem.*, 1998, **87**, 87; C. Bartolomé, P. Espinet, F. Villafañe, S. Giesa, A. Martín and A. G. Orpen, *Organometallics*, 1996, **15**, 2019; K. B. Dillon, V. C. Gibson, J. A. K. Howard, L. J. Sequeira and J. W. Yao, *Polyhedron*, 1996, **15**, 4173; V. C. Gibson, C. Redshaw, L. J. Sequeira, K. B. Dillon, W. Clegg and M. R. J. Elsegood, *Chem. Commun.*, 1996, 2151; K. B. Dillon, V. C. Gibson, J. A. K. Howard, C. Redshaw, L. Sequeira and J. W. Yao, *J. Organomet. Chem.*, 1997, **528**, 179; M. G. Davidson, K. B. Dillon, J. A. K. Howard, S. Lamb and M. D. Roden, *J. Organomet. Chem.*, 1998, **550**, 481; P. Espinet, S. Martín-Barrios, F. Villafañe, P. G. Jones and A. K. Fisher, *Organometallics*, 2000, **19**, 290; A. S. Batsanov, K. B. Dillon, V. C. Gibson, J. A. K. Howard, L. J. Sequeira and J. W. Yao, *J. Organomet. Chem.*, 2001, **631**, 18; A. S. Batsanov, S. M. Cornet, L. A. Crowe, K. B. Dillon, R. K. Harris, P. Hazendonk and M. D. Roden, *Eur. J. Inorg. Chem.*, 2001, 1729.

2 K. B. Dillon, H. P. Goodwin, T. A. Straw and R. D. Chambers, *Euchem. Conf. Phosphorus, Silicon, Boron and Related Elements in Low Coordinated States*, Paris-Palaiseau, 1988.

3 K. H. Whitmire, D. Labahn, H. W. Roesky, M. Noltemeyer and G. M. Sheldrick, *J. Organomet. Chem.*, 1991, **402**, 55.

4 J. K. Buijink, M. Noltemeyer and F. T. Edelmann, *J. Fluorine Chem.*, 1993, **61**, 51.

5 N. Burford, C. L. B. Macdonald, D. J. LeBlanc and T. S. Cameron, *Organometallics*, 2000, **19**, 152.

6 R. D. Schluter, H. S. Isom, A. H. Cowley, D. A. Atwood, R. A. Jones, F. Olbritch, S. Corbelin and R. J. Lagow, *Organometallics*, 1994, **13**, 4058.

7 R. D. Schluter, A. H. Cowley, D. A. Atwood, R. A. Jones, M. R. Bond and C. J. Carrano, *J. Am. Chem. Soc.*, 1993, **115**, 2070.

8 M. Bardají, P. G. Jones, A. Laguna, A. Moracho and A. K. Fischer, *J. Organomet. Chem.*, 2002, **648**, 1.

9 K. Ishihara, S. Ohara and H. Yamamoto, *J. Org. Chem.*, 1996, **61**, 4196.

10 K. Ishihara, M. Mouri, Q. Gao, T. Maruyama, K. Furuta and H. Yamamoto, *J. Am. Chem. Soc.*, 1993, **115**, 11490.

11 V. C. Gibson, C. Redshaw, W. Clegg and M. R. J. Elsegood, *Polyhedron*, 1997, **16**, 2637.

12 W. Fraenk, T. M. Klapötke, B. Brumm, P. Mayer, H. Nöth, H. Piotrowski and M. Suter, *J. Fluorine Chem.*, 2001, **112**, 73.

13 A. Pelter, K. Smith and H. C. Brown, *Borane Reagents: Best Synthetic Methods*, Academic Press, London, 1988, p. 428.

14 K. Sasakura, Y. Terui and T. Sugasawa, *Chem. Pharm. Bull.*, 1985, **33**, 1836.

15 H. J. Frohn, H. Franke, P. Fritzen and V. V. Bardin, *J. Organomet. Chem.*, 2000, **598**, 127.

16 R. Duchateau, S. J. Lancaster, M. Thornton-Pett and M. Bochmann, *Organometallics*, 1997, **16**, 4995.

17 R. L. Giles, J. A. K. Howard, L. G. F. Patrick, M. R. Probert, G. E. Smith and A. Whiting, *J. Organomet. Chem.*, 2003, **680**, 257.

18 A. S. Batsanov, S. M. Cornet, K. B. Dillon, A. E. Goeta, A. L. Thompson and B. Y. Xue, *Dalton Trans.*, 2003, 2496.

19 *Thermodynamical Properties of Individual Substances*, ed. I. V. Gurvich, I. V. Veits and S. B. Alcock, Hemisphere Publ. Corp., Washington DC, USA, 4th edn., 1991, vol. 2, pt. 1; *Handbook of Chemistry and Physics*, ed. D. R. Lide, CRC Press, Boca Raton, FL, USA, 76th edn., 1995–1996; S. S. Batsanov, *Strukturnaya Khimiya*, Dialog MGU, Moscow, 2000.

20 M. E. Schwarz and L. C. Allen, *J. Am. Chem. Soc.*, 1970, **92**, 1466.

21 S. Toyota, M. Asakura, M. Ōki and F. Toda, *Bull. Chem. Soc. Jpn.*, 2000, **73**, 2357.

22 A. S. Batsanov, S. M. Cornet, K. B. Dillon, A. E. Goeta, P. Hazendonk and A. L. Thompson, *J. Chem. Soc., Dalton Trans.*, 2002, 4622.

23 K. J. Weese, R. A. Bartlett, B. D. Murray, M. M. Olmstead and P. Power, *Inorg. Chem.*, 1987, **26**, 2409.

24 W. E. Piers, R. E. v. H. Spence, L. R. MacGillivray and M. J. Zaworotko, *Acta Crystallogr., Sect. C*, 1995, **51**, 1688.

25 W. V. Konze, B. L. Scott and G. J. Kubas, *Chem. Commun.*, 1999, 1807.

26 J. F. Blount, P. Finocchiaro, D. Gust and K. Mislow, *J. Am. Chem. Soc.*, 1973, **95**, 7019.

27 D. C. Bradley, I. S. Harding, A. D. Keefe, M. Motevalli and D. H. Zheng, *J.Chem. Soc., Dalton Trans.*, 1996, 3931.

28 M. T. Reetz, J. Huff, J. Rudolph, K. Töllner, A. Deeze and R. Goddard, *J. Am. Chem. Soc.*, 1994, **116**, 11588.

29 W. J. Evans, J. L. Shreeve and J. W. Ziller, *Acta Crystallogr., Sect. C*, 1996, **52**, 2571; M. Niehues, G. Erker, O. Meyer and R. Frohlich, *Organometallics*, 2000, **19**, 2813.

30 W. I. Cross, M. P. Lightfoot, F. S. Mair and R. G. Pritchard, *Inorg. Chem.*, 2000, **39**, 2690.

31 K. R. Leopold, M. Canagaratna and J. A. Phillips, *Acc. Chem. Res.*, 1997, **30**, 57.

32 H. Jiao and P. v. R. Schleyer, *J. Am. Chem. Soc.*, 1994, **116**, 7429.

33 V. Jonas, G. Frenking and M. T. Reetz, *J. Am. Chem. Soc.*, 1994, **116**, 8741.

34 B. D. Bowsell, R. J. Gillespie and G. L. Heard, *Inorg. Chem.*, 1999, **38**, 4659.

35 J. Cosier and A. M. Glazer, *J. Appl. Crystallogr.*, 1986, **19**, 105.

36 SMART-NT, Data Collection Software, version 5.0, Bruker Analytical X-ray Instruments Inc., Madison, WI, 1999.

37 SAINT-NT, Data Reduction Software, version 6.0, Bruker Analytical X-ray Instruments Inc., Madison, WI, 1999.
38 SHELXTL, version 5.1, Bruker X-ray Analytical Instruments Inc., Madison, WI, 1999.
39 M. J. Frisch, G. W. Trucks, H. B. Schlegel, G. E. Scuseria, M. A. Robb, J. R. Cheeseman, V. G. Zakrzewski, J. A. Montgomery, Jr., R. E. Stratmann, J. C. Burant, S. Dapprich, J. M. Millam, A. D. Daniels, K. N. Kudin, M. C. Strain, O. Farkas, J. Tomasi, V. Barone, M. Cossi, R. Cammi, B. Mennucci, C. Pomelli, C. Adamo, S. Clifford, J. Ochterski, G. A. Petersson, P. Y. Ayala, Q. Cui, K. Morokuma, D. K. Malick, A. D. Rabuck, K. Raghavachari, J. B. Foresman, J. Cioslowski, J. V. Ortiz, B. B. Stefanov, G. Liu, A. Liashenko, P. Piskorz, I. Komaromi, R. Gomperts, R. L. Martin, D. J. Fox, T. Keith, M. A. Al-Laham, C. Y. Peng, A. Nanayakkara, C. Gonzalez, M. Challacombe, P. M. W. Gill, B. G. Johnson, W. Chen, M. W. Wong, J. L. Andres, M. Head-Gordon, E. S. Replogle and J. A. Pople, GAUSSIAN 98 (Revision A.9), Gaussian, Inc., Pittsburgh, PA, 1998.
40 T. P. Onak, H. L. Landesman and R. E. Williams, *J. Phys. Chem.*, 1959, **63**, 1533.
41 T. Onak, M. Diaz and M. Barfield, *J. Am. Chem. Soc.*, 1995, **117**, 1403.
42 M. A. Fox, R. Greatrex and D. L. Ormsby, *Chem. Commun.*, 2002, 2052.